2019

Investigating potential barium sources at Mormon Mesa, Nevada: an integrated geochemical-geomorphological study

India Futterman
Vassar College

Investigating potential barium sources at Mormon Mesa, Nevada: An integrated geochemical-geomorphological study

India Futterman
Earth Science
May 2019

Senior Thesis

Advisors: Kirsten Menking; Colin R. Robins

Table of Contents

ABSTRACT

The Mormon Mesa soil series, one of the world's oldest and best-preserved petrocalcic soils, represents the product of continuous accumulation of atmospherically-sourced ions within the Muddy Creek Formation parent material, deposited in the Pliocene epoch. Because the translocation of atmospherically-sourced ions is largely dependent on climate conditions and the geomorphological processes these conditions give rise to, the presence of certain elements and mineral phases in the Mormon Mesa soil series may be used as proxies for both paleoclimate conditions and geomorphological processes. The goal of this study was to determine the source of barium ions at Mormon Mesa to explain the presence of authigenic barite in the uppermost horizons of the soil sequence. Authigenic barite is somewhat anomalous at Mormon Mesa given that barium and barite are typically insoluble in arid conditions; however, experimental results indicate that Ba^{+} ions can be mobilized in the presence of certain other ions. Barium ions may be atmospherically-sourced and transported by wind and precipitation to the mesa surface; alternatively, Ba^{+} ions may have been derived from parent material. Chemical analyses of surface and profile samples returned the highest Ba values in the uppermost horizons of the soil series. This supports the atmospherically-sourced hypothesis, since ion inputs at the surface of the mesa would be mainly sequestered in the upper regions of the profile. Additionally, relatively high Ba levels detected among surface drainage network samples may indicate additional hydrological influences in the barium mobilization pathway.

ACKNOWLEDGEMENTS

This material is based upon work supported by the Keck Geology Consortium and the National Science Foundation under Grant No. 1659322. Special thanks to Colin R. Robins, Penelope Vorster, Ethan Conley, and Kurt Crandall for their support in the field and laboratory. Major support from the Keck Geology Consortium was provided by Cam Davidson, Karl Wirth, Marga Miller, and Jonathan Harris. This project would not have been possible without the advising of Kirsten Menking and Jeff Walker in the Vassar College Earth Science Department. Other Vassar staff involved in this project include Rick Jones, and Joseph Tanski. Neil Curri provided invaluable assistance with GIS operations. Special thanks to Dr. Karen Wovkulich for her patient help with ICP and XRF analyses. Thanks also to Amy Brock-Hon for her foundational research on barite in Mormon Mesa soils. Matthew Rahn Manon and the Union College Department of Geology provided access to laboratory space and use of Union College's handheld XRF. Permission to sample was provided by the Clark County Bureau of Land Management through a letter of understanding (680 NVS0100).

INTRODUCTION

About fifty miles northeast of Las Vegas in the Mojave Desert of southeastern Nevada lies Mormon Mesa, a broad, roughly triangular landform flanked by the Muddy (west) and Virgin (east) Rivers (Fig. 1). The mesa is composed of an ancient petrocalcic soil developed in the Pliocene-age sediments of the Muddy Creek Formation. The product of 4-5 million years of secondary calcium carbonate accumulation in a tectonically stable region, the Mormon Mesa soil series is one of the oldest intact petrocalcic soils in the world. Calcic soils are defined by their significant enrichment of calcium carbonate, most often concentrated in an upper region of the soil profile known as the calcic horizon (Machette, 1985). The prefix "petro" denotes the complete induration of the calcic horizon due to extensive $CaCO_3$ accumulation over time (Robins et al., 2012). Due to the high susceptibility of calcium carbonate to chemical weathering, these soils are generally restricted to arid regions such as the basins of the American southwest, the climate of which permits the continuous accumulation of atmospherically-sourced ions over time (Machette, 1985). The rate and extent of atmospherically-sourced ion input varies between pluvial/glacial and interpluvial/interglacial climate cycles, as different amounts of meteoric precipitation affect the rate of translocation as well as the ionic strength of the translocated solutions. As such, the

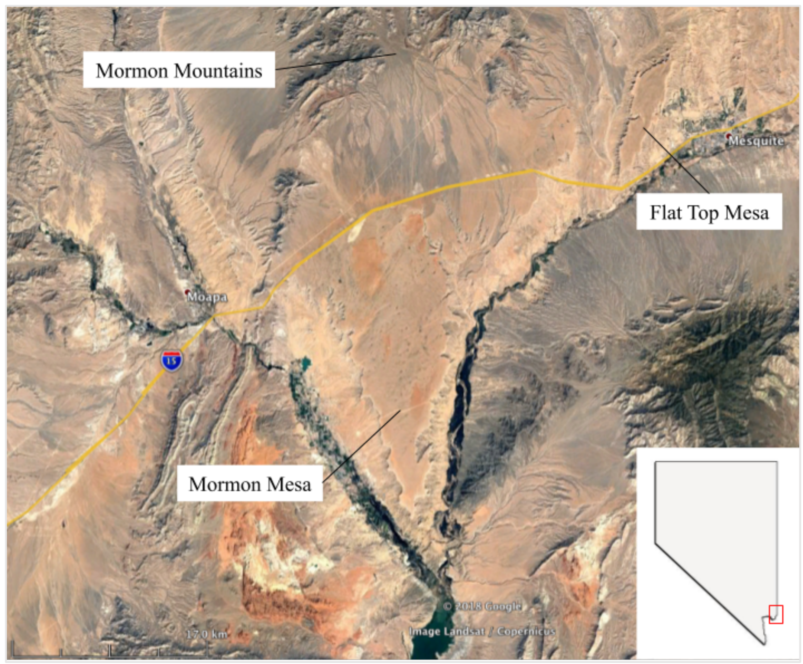

Figure 1: Study site (Imagery: Google Earth).

minerals present in petrocalcic soils can be interpreted as the products of specific climate conditions, and petrocalcic soil geochemistry can be used in paleoclimate reconstructions. Mormon Mesa is particularly well-suited to this task, not only because it is so well-preserved, but also because it developed in an almost carbonate-free substrate, so its calcium carbonate content serves as an accurate indicator of the extent of atmospheric ion inputs (Gardner, 1972).

Mormon Mesa is also an example of a relict soil, one that has formed continuously since its parent material was deposited (Robins et al., 2012). Thus, the story of the Mormon Mesa petrocalcic soil begins with the deposition of its parent material, the Muddy Creek Formation, during the Pliocene epoch (Gardner, 1972). The Muddy Creek formation is composed mainly of fluvial and alluvial siliciclastic sediments and includes volcanic and plutonic clasts as well as lacustrine sediments, siltstones, and evaporites (Scott, 1988). Today, the relatively unaltered Muddy Creek formation can be seen at Mormon Mesa (Fig. 2) at the lowermost horizon in exposed soil profiles and is composed mainly of friable red siliceous sand.

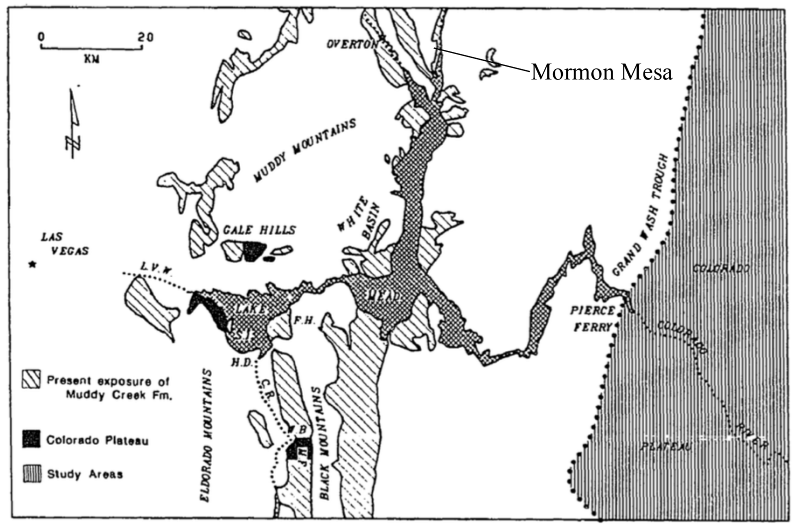

Figure 2: Present exposures of the Muddy Creek Formation (from Scott, 1988). Triangular landform north of Lake Mead is Mormon Mesa.

Calcic soil development commenced following deposition of Muddy Creek sediments. While several potential mechanisms exist to explain ion dissolution and translocation through the Muddy Creek parent material, atmospheric sourcing of ions and their subsequent dissolution in rainwater and percolation through parent sediments is generally accepted as the primary

Figure 3: Potential regional playa dust sources (blue stars). Red star denotes playa sampled in this study (Imagery: Landsat/Copernicus, Google Earth).

mechanism for ion inputs at Mormon Mesa (Machette, 1985; Gardner, 1972). Several lines of evidence support the atmospheric sourcing theory. Ion sourcing from groundwater is unlikely given the appreciable depth of the water table relative to the mesa surface as well as the low capillary rise potential of Muddy Creek sediments (Machette, 1985). Careful inspection of detrital parent material grains in the most well-indurated regions of the Mormon Mesa soil sequence reveal little to no evidence of weathering, indicating that dissolution of parent material is not a primary ion input mechanism within this soil (Gardner, 1972). Additionally, and perhaps most importantly, there are an abundance of dry playas adjacent to Mormon Mesa, the dust from which is easily entrained by wind and has very likely been continuously deposited in the Mormon Mesa area (see Fig. 3).

Dust flux is considered a significant soil-forming process in arid regions such as the Mojave Desert (Reheis, 2006), due in large part to the fact that these soils contain sediments and minerals not present or weatherable from their parent materials, which must therefore be distally sourced (Reheis et al., 1995). Regionally, dust is generated from both alluvial and playa sources, and its eolian entrainment and transport is intensified during dry climate cycles, when sediments are highly unconsolidated and vegetation is at a minimum (Reheis, 2006). The systematic decrease in concentration of such elements as arsenic and antimony as far as 400 km downwind of the Owens Lake dust source site (at which arsenic and antimony levels are high) indicates active dust transport from playas (Reheis et al., 2002).

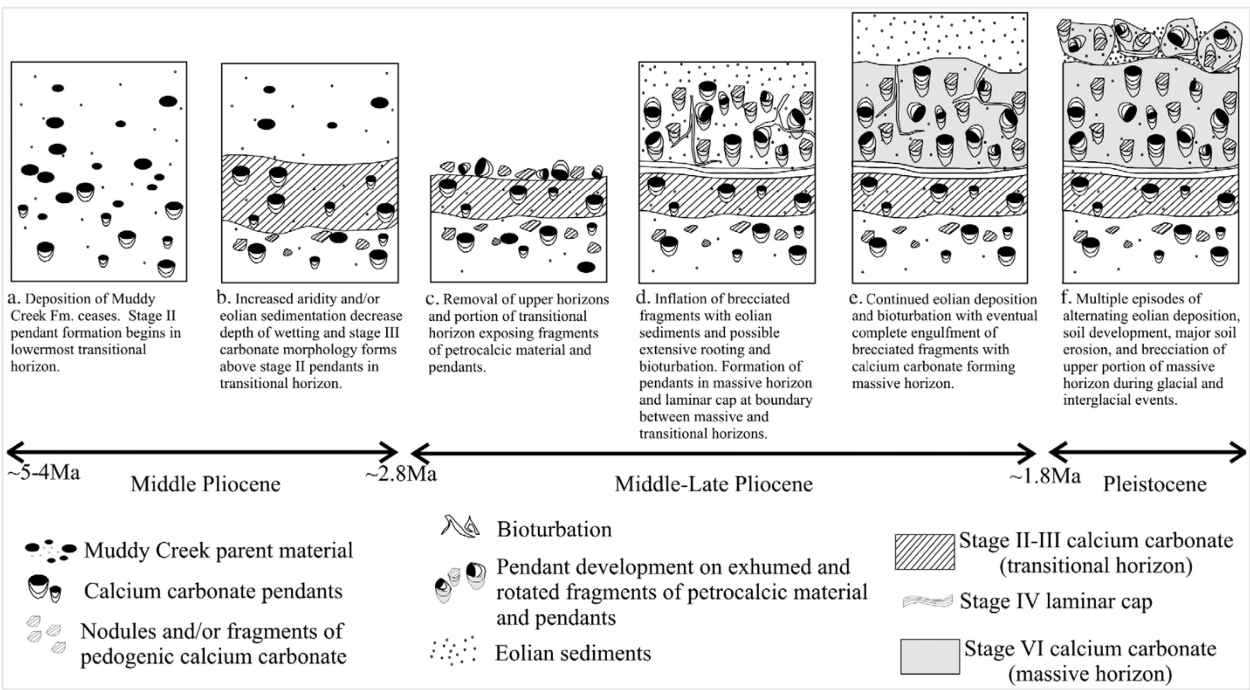

Figure 4: Modified six-stage calcic soil development model for Mormon Mesa (from Brock and Buck, 2009)

Here it becomes necessary to introduce the generalized six-stage calcic soil development model (Machette, 1985; see Fig. 4). With the continuous accumulation of ions over time combined with erosional events and climate cycles, a distinct, age-diagnostic assemblage of micromorphological features forms within calcic soils. Some of these features include pendants - concentric, sometimes rotated, stalactitic/ooilitic $CaCO_3$ accumulations on the undersides of lithic fragments or other nuclei; laminations – thin, alternating bands of mineral precipitates resulting from hydrological activity; and nodules – round, clast-like concentrations of calcium carbonate embedded throughout the profile (see Fig. 5). Stage I, the least-developed calcic soil phase, is defined by minimal calcium carbonate accumulation, usually present as thin coatings on detrital clasts. Stage II horizons may contain calcium carbonate nodules and thicker accumulations of carbonate on detrital clasts. Stage III development marks the early stages of calcium carbonate cementation. Development of carbonate laminae in the upper portion of the profile begins at Stage IV (Fig. 5, top) and increases in Stage V, which is also distinguished by the presence of calcic pendant growth around detrital clast nuclei (Fig. 5, bottom). Finally, Stage VI development is defined by an extremely high degree of cementation/induration, abundant laminae and pendants, as well as the presence of reworked, recemented fragments of indurated material following multiple erosional events (Machette, 1985).

Figure 4: Cut hand samples of massive horizon featuring laminae (top) and pendants (bottom).

The Mormon Mesa soil sequence has been divided into four distinct horizons, each of which display different degrees of development based on the six-stage model (see Figs. 6 and 7). The bottommost horizon is composed of relatively unaltered, loosely compacted red sandstone (Muddy Creek Formation sediments), displaying, at most, Stage I morphology. Above this sits the thick transitional horizon, which at some exposures can be divided into lower, middle, and upper horizons distinguished by varying degrees of calcium carbonate accumulation as well as the presence of nodules and other micromorphological features. Generally, the transitional zone displays Stage III calcic soil development and is weakly consolidated with a powdery texture. Above the transitional horizon sits the highly indurated, Stage VI massive horizon, in which abundant laminae, pendants, and reworked fragments can be seen. The uppermost horizon is a thin (not exceeding about 15 cm in most locations) layer of reworked, unconsolidated massive horizon fragments and recently deposited detrital fragments, dust, and alluvium. Overall, there is a downward decreasing trend in cementation/induration throughout the Mormon Mesa profile (Gardner, 1972). The modern mesa surface is composed of moderately vegetated unconsolidated sandy sediments, which in some locations are overlain by thin biological crusts. The surface is also mantled by sand dunes and is affected by ephemeral hydrological activity, evidenced by vegetated drainage networks, depression pits in which water collects sporadically, and arroyos.

Figure 5: The complete Mormon Mesa soil profile, Flat Top Mesa East. 1 = rubble horizon; 2 = massive, 3 = upper transitional; 4 = middle transitional; 5 = lower transitional; 6 = Muddy Creek Formation with minor calcium carbonate accumulation; 7 = mostly unaltered Muddy Creek material. All profiles display slightly variable horizon morphology.

Besides their distinct micromorphological characteristics, the mineralogical makeup of the Mormon Mesa soil horizons can also provide insight into influential climatic and geomorphic processes. One of the most confounding minerals identified in scanning electron microscopy (SEM) imagery of samples from the massive and transitional horizons is authigenic barite, $BaSO_4$ (Brock-Hon et al., 2012; see Fig. 8). The presence of barite crystals grown in-situ in Mormon Mesa soil is unexpected given the insolubility of barium and barite in arid environments (Brock-Hon et al., 2012). Typically, authigenic barite in soils is only found in anoxic, hydromorphic, low pH, reducing conditions with high base saturation – in other words, in warm, humid climes (Darmody et al., 1989; Stoops and Zavaleta, 1978). However, experimental laboratory results indicate that the solubility of barium increases linearly with increasing NaCl and Mg^{2+} concentration (Blount, 1977; Deutsche, 1997). Given the broad range of ion inputs in the Mormon Mesa soil, it is probable that Ba^{+} ions were mobilized in the presence of NaCl or Mg^{2+} and were subsequently able to combine with SO_4^{-} ions to form authigenic barite crystals.

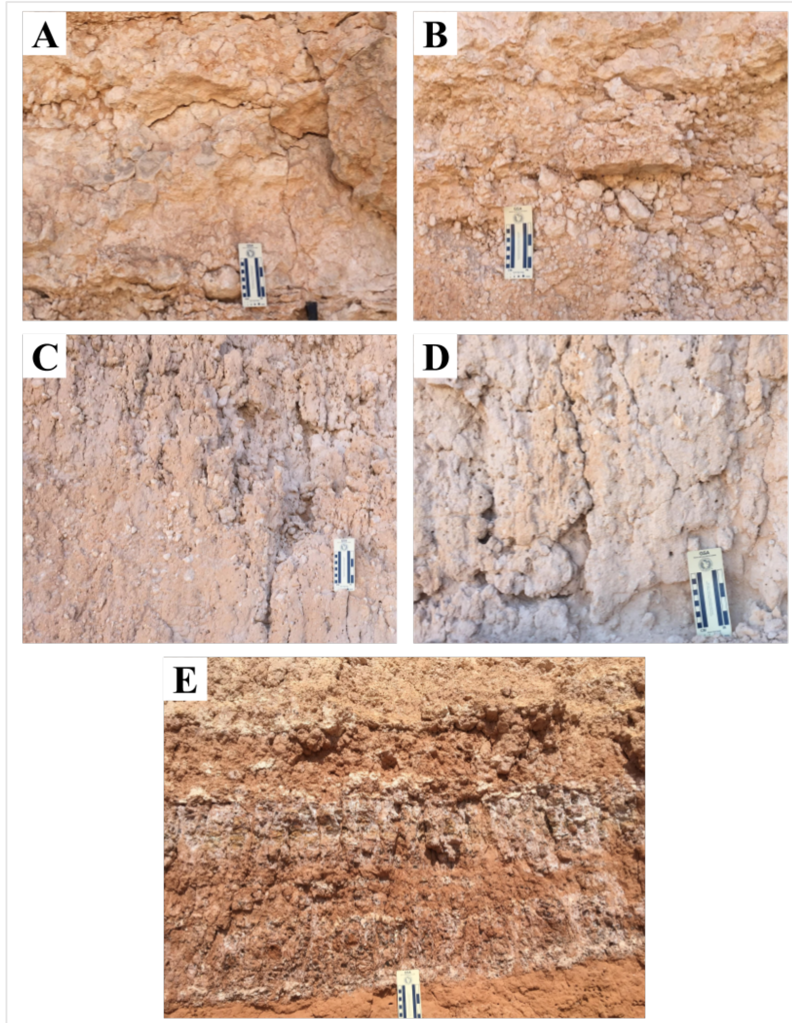

Figure 6: Detailed horizon photos, Flat Top Mesa East. A = massive; B = upper transitional; C = middle transitional; D = lower transitional; E = Muddy Creek Formation with minor calcium carbonate accumulation.

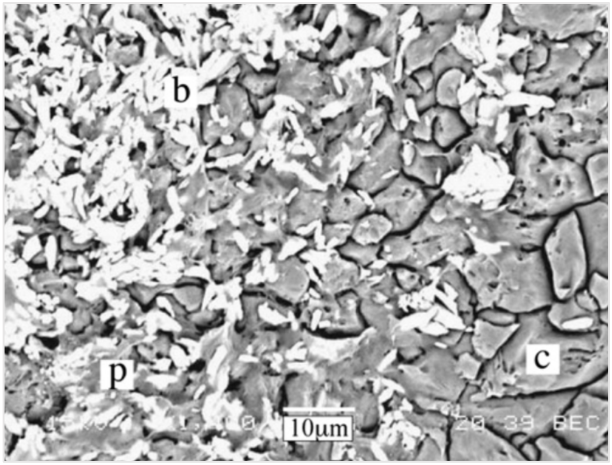

Figure 7: SEM backscatter imagery of authigenic barite crystals in massive horizon sample from Overton profile site, Mormon Mesa (from Brock-Hon et al., 2012). Barite crystals labeled "b". The orientation and euhedral shape of these barite grains indicates that they are authigenic rather than transported.

Currently, a conceptual model exists explaining this ion mobilization pathway in interpluvial and pluvial climate cycles (Robins et al., 2012). During arid, interpluvial climate periods, the rarity of precipitation events is thought to increase the ionic strength of atmospherically-sourced ion solutions entering the soil. These ion solutions, bearing, among other elements, Na^{2+}, Cl^{-}, Mg^{2+}, and Ba^{2+}, percolate through and saturate the massive horizon. The presence of Na^{2+}, Cl^{-}, and Mg^{2+} increases the solubility of Ba^{2+} in solution, mobilizing Ba^{2+} ions and allowing them to react with SO_4^{2-} ions in solution to precipitate authigenic barite crystals once the solution is saturated. Additionally, the consumption of Mg^{2+} ions in the formation of fibrous clays drives the precipitation of insoluble, authigenic barite crystals. In subsequent pluvial periods, the ionic strength of rainwater/ion solutions is decreased due to the increased frequency of rainfall. As such, the ionic strength of Na^{2+}, Cl^{-}, and Mg^{2+} is too low to re-mobilize Ba^{2+} and SO_4^{-} ions in the authigenic barite, so the crystals remain intact in the substrate (Robins et al., 2012). Published elemental data (Robins et al., 2012) support this model: in generally, the highest Ba values detected in the massive and transitional horizons (745-1716 ppm) roughly correspond with high Na values (351-673 ppm). A positive correlation between Mg and Ba concentrations is less apparent.

The primary source of the barium ions involved in barite authigenesis at Mormon Mesa remains unidentified. Two possible sources present themselves: dissolution of the Muddy Creek parent material, or atmospheric inputs from dust flux. As discussed above, dust flux is recognized as a highly influential geomorphological and soil forming process in the American Southwest. Geochemical analysis of dust from various regional playas reveals barium levels ranging from 487-3750 ppb, and Na mass percent values of up to 3.9% (Reheis et al., 2002). The highest Ba levels have been detected in dust from nearby Owens Lake, which is known to transport dust up to 400 km to the east (Reheis et al., 2002). Mormon Mesa lies within 300 km to the east of Owens Lake, and as such, has likely received dust inputs from the dry lakebed. However, prevailing winds in the area currently travel in the northeast direction (National Digital Forecast Database, 2019), so modern dust inputs are likely sourced from a different set of playas, the elemental composition of which may or may not resemble that of the Owens Lake bed. Furthermore, prevailing wind direction has certainly shifted innumerable times since the beginning of Mormon Mesa soil development, meaning that a large diversity of dust sources has likely contributed to the mineralogical makeup of the soil sequence. Besides playa dust, barium may also be derived from desert varnish, a weathering product that often develops on rock surfaces in arid environments and which may be broken down and transported by eolian forces. Desert varnish often contains hollandite, a magnesium oxide mineral in which barium is typically present (Garvie et al. 2008).

Despite abundant evidence from published studies of Mormon Mesa soil development and regional dust flux to support the atmospherically-sourced ion hypothesis, parent material sourcing must also be considered as a possibility for barium ion input. The Muddy Creek sediments contain igneous clasts that may include potassium feldspar and micas, two minerals in which Ba^+ ions have been known to substitute for K^+. Additionally, Ba^+ may infrequently substitute for Ca^{2+} in amphibole, plagioclase feldspar, and pyroxene, minerals that may also be present in the Muddy Creek Formation (Johnson et al., 2017; Scott, 1988).

The goal of this study is to identify the most likely source of barium ions, which may reveal the nuances of chemical mobilization pathways fundamental to the development of all soils. Additionally, this study may illuminate processes by which authigenic barite occurs in other calcic soils of the world. Mapping elemental concentrations across the mesa surface and throughout soil profiles may show wind-driven variations in geochemistry and reveal potential correlation with geomorphic processes responsible for the creation of drainages and depression pits. Specifically, a downwind-directional decrease in Ba concentration would suggest a primarily eolian source for Ba. Conversely, lack of variability of Ba between horizons or across the mesa surface could support a parent material source.

METHODS

Map unit description

A geomorphic map of the mesa surface was created based on remote sensing interpretations, field observations, and using the image classification spatial analyst tool in ArcMap (USDA-FSA-APFO 2017; see Fig. 9). Five prominent geomorphic units were defined: sand dunes - modern eolian features composed primarily of red quartz sand; gullies - dendritic, vegetated, intermittently wetted subsurface drainage networks; depression pits - the round, vegetated, water collection points of gully drainages; arroyos - ephemerally wet stream beds actively eroding inwards from the edges of the mesa; and undifferentiated mesa surface, defined as sparsely vegetated eolian sands mantling alluvial fan gravels.

Surface site locations and sampling

Field work for this study was conducted in June, 2018. Eighty-six samples were collected in total; of these, 55 were analyzed using inductively coupled plasma mass spectrometry (ICP-MS). Two groups of surface samples were collected: geomorphic unit samples and transects. Geomorphic samples were collected to ensure adequate representation of the mesa surface in the dataset and to assess the influence of geomorphic processes on soil geochemistry. Transect samples were collected for a systematic study of surface geochemistry variability, especially as this variability relates to eolian dust flux. 200-1000 g of substrate were collected at each sampling site. Two arroyos, two sand dunes, three depression pits, and two drainage gullies were sampled at Mormon Mesa. Additionally, one sand dune and three depression pits were sampled at adjacent Flat Top Mesa, a separate, isolated remnant of the once more continuous paleo-Mormon Mesa soil geomorphic surface. Twenty samples were collected parallel to the northernmost road on Mormon Mesa, at a distance of 0.2 km north of the road and at intervals of approximately 0.5 km along the transect. Of these 20 samples, 12 were analyzed using ICP-MS. Ten samples were collected along a transect parallel to a shorter, more southern Mormon Mesa road, at 0.2 km south of the road and at intervals of approximately 0.4 km along the transect; five of these samples were analyzed. Eight samples were collected along a Flat Top Mesa transect at intervals of approximately 0.25 km; six of these were analyzed.

Profile locations and sampling

Two complete soil profiles were sampled at both Mormon Mesa (Riverside and Overton sites, respectively located on the east and west edges of the mesa) and Flat Top Mesa (Flat Top East and Flat Top West; see Fig. 12). The Riverside and Overton sites are well-studied (Brock-Hon et al. 2012; Robins et al 2012), whereas neither Flat Top Mesa profile had been sampled prior to this study. 200-1000 g of substrate were collected from each soil horizon: Muddy Creek parent material; lower, middle, and upper transitional subhorizons; massive; and rubble.

Laboratory preparation and geochemical analysis

Unconsolidated samples (e.g., all surface samples) were sieved to separate the fine fraction (>2 mm) from large organic matter and clasts. The coarse fraction, largely or entirely composed of petrocalcic fragments, was retained. Indurated or partially cemented samples (e.g., all petrocalcic horizon samples) were pulverized in steel rock chippers and disc mills to achieve fine fractionation. Fifty-five representative samples were chosen for ICP-MS analysis. 0.5 g of each of the 55 selected samples was digested using EPA Method 3050b, Section 7.5 (see Appendix A). Al, Mn, K, and Ba levels were analyzed for all samples using a 16x dilution (625µL in 10 mL 1% nitric acid solution). Mg levels were analyzed for selected samples using a 200x dilution (50µL in 10 mL 1% nitric acid solution). Na could not be measured due to time constraints. Dilution levels for this experiment were chosen based on published elemental concentrations in Mormon Mesa soil samples (Robins et al., 2012). Digests were analyzed for elemental content using a Thermo Scientific iCapRQ ICP-MS run in KED mode housed in the Chemistry Department of Vassar College. Three elemental standards were used to create the calibration curve for ICP analysis: SRM 2586, WPS1, and WPS3 (see Appendix B for standard elemental concentrations).

RESULTS

Four samples tested were removed from the data analysis due to ICP-MS run errors that produced inaccurate results. Elemental data from the remaining 51 samples tested are presented in Tables 1-3 below. All geomorphic sample values (Table 1) and transect sample values (Table

2) were plotted on maps of both Mormon and Flat Top Mesa surfaces (Figs. 10, 11). Depression pit samples contained the highest measured concentrations of Ba among all geomorphic features sampled (42.44-72.85 ppb; see Figs. 10 and 11, Table 1). One drainage gully sample also returned elevated Ba levels (48.39 ppb; see Fig. 12, Table 1). The single playa sample was relatively abundant in Ba (50.48 ppb) whereas Ba concentrations between the two arroyo samples tested ranged from low (12.79 ppb) to moderate (30.16 ppb).

Table 1: Selected elemental concentrations (ppb) from ICP-MS analysis of geomorphic feature samples from Mormon Mesa and Flat Top Mesa.

Sample Code	Sample Type	Location	Mn	Ba	Fe	K	Al	Mg
FTM2018IFP2I	Depression	Flat Top Mesa	75.58	42.43	2946.28	372.17	2080.57	57.21
FTM2018IFSD	Sand Dune	Flat Top Mesa	12.59	4.69	844.36	14.68	345.43	1.97
A2018IF1	Arroyo	Mormon Mesa	753.81	12.79	1193.06	142.75	571.27	177.14
MM2018IFDG1	Drainage Gully	Mormon Mesa	98.78	48.39	3501.64	557.65	2610.98	66.87
MM2018IFDG2	Drainage Gully	Mormon Mesa	78.03	35.92	2855.12	394.62	1894.83	42.61
MM20108IFP1I	Depression	Mormon Mesa	119.83	69.70	4289.36	912.06	3808.70	126.43
MM2018IFA2	Arroyo	Mormon Mesa	36.88	30.16	2056.70	210.90	1483.18	37.95
MM2018IFP3	Depression	Mormon Mesa	95.77	50.00	3528.28	558.79	2738.23	67.94
MM2018IFP4	Depression	Mormon Mesa	114.80	72.85	4268.03	863.83	3693.18	123.88
MM2018IFSD2b	Sand Dune	Mormon Mesa	18.59	6.75	1475.05	87.13	559.90	4.32
MMO2018IFSD	Sand Dune	Mormon Mesa	16.32	4.83	1139.15	16.87	282.58	1.85
MMTN2018SD2	Sand Dune	Mormon Mesa	31.77	8.52	2917.76	62.34	620.34	11.07

Table 2: Selected elemental concentrations (ppb) from ICP-MS analysis of transect samples. "Transect Location" number corresponds to distance along transect (1 = westernmost, 12 = easternmost).

Sample Code	Transect Location	Mn	Ba	Fe	K	Al
FTM2018IFT1	1	68.47	31.00	2998.96	656.04	1896.16
FTM2018IFT2	2	26.95	6.49	1227.59	332.63	718.37
FTM2018IFT3	3	30.03	7.11	1247.93	354.37	720.84
FTM2018IFT5	4	44.74	16.99	2302.77	725.55	1403.09
FTM2018IFT7	5	51.76	18.88	2763.60	930.34	1727.99
FTM2018IFT8	6	92.17	27.57	2979.17	767.33	2002.83
MMTN2018IF1	1	32.67	14.03	2071.36	114.95	919.56
MMTN2018IF2	2	139.75	28.33	3195.24	1162.89	2358.61
MMTN2018IF4	3	56.13	21.73	2991.75	961.22	1841.91
MMTN2018IF6	4	82.38	28.54	3221.19	1324.74	2832.37
MMTN2018IF8	5	73.12	24.52	3158.94	1295.36	2303.55
MMTN2018IF10	6	74.71	25.17	3232.00	1124.95	2168.13
MMTN2018IF12	7	71.23	24.38	3360.50	1179.38	2083.72
MMTN2018IF14	8	56.21	21.39	3152.53	882.00	1778.80
MMTN2018IF16	9	75.25	23.65	3073.52	1104.00	2216.31
MMTN2018IF18	10	66.66	24.19	3092.57	1221.45	1988.83
MMTN2018IF20	11	87.07	31.07	3313.34	1290.22	2902.44
MMTN2018IF23	12	70.49	48.21	3046.29	326.75	2095.99
MMTS2018IF2	1	27.52	9.79	1653.60	433.06	948.86
MMTS2018IF4	2	55.24	23.39	3057.97	985.47	2120.40
MMTS2018IF6	3	72.51	26.57	2899.30	1083.91	2051.15
MMTS2018IF8	4	54.27	20.72	2952.13	935.53	1900.12
MMTS2018IF10	5	46.27	17.34	2582.70	787.01	1449.09

Elemental analyses of transect samples present no apparent spatial trends in terms of increasing or decreasing Ba concentration (Figs. 11 and 12; Table 2). High concentrations of Ba were found at both ends of the Flat Top Mesa transect: the easternmost sample returned a value of 27.57 ppb, the westernmost sample 31.00 ppb (minimum transect value: 6.50 ppb). The majority of samples along the northern Mormon Mesa transect ranged between 21.00 and 25.00 ppb, with a notable exception at the easternmost end of the transect (48.21 ppb). Ba concentrations peaked at the middle of the southern Mormon Mesa transect (26. 57 ppb; min. 9.79 ppb).

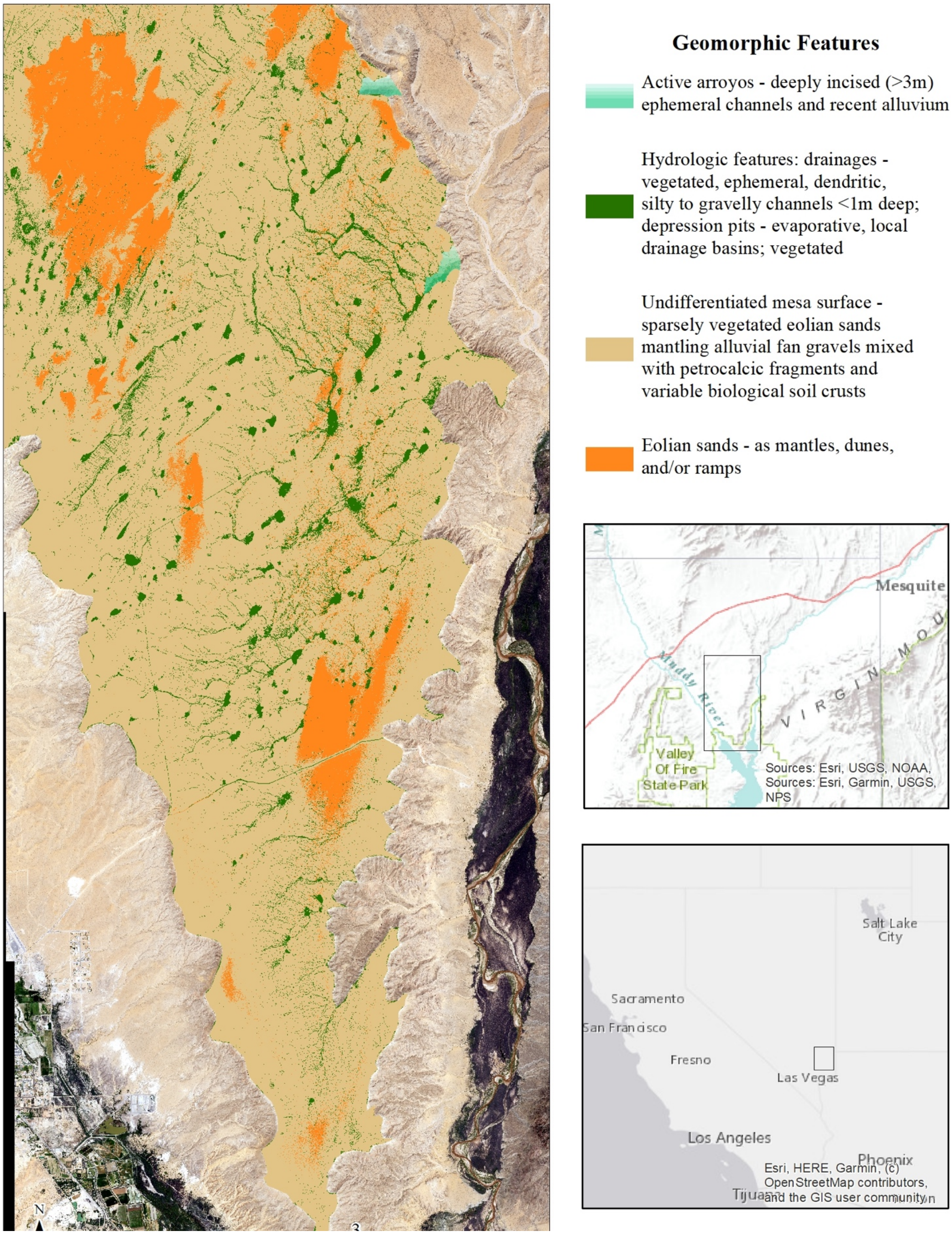

Figure 9: Geomorphic map of modern Mormon Mesa surface.

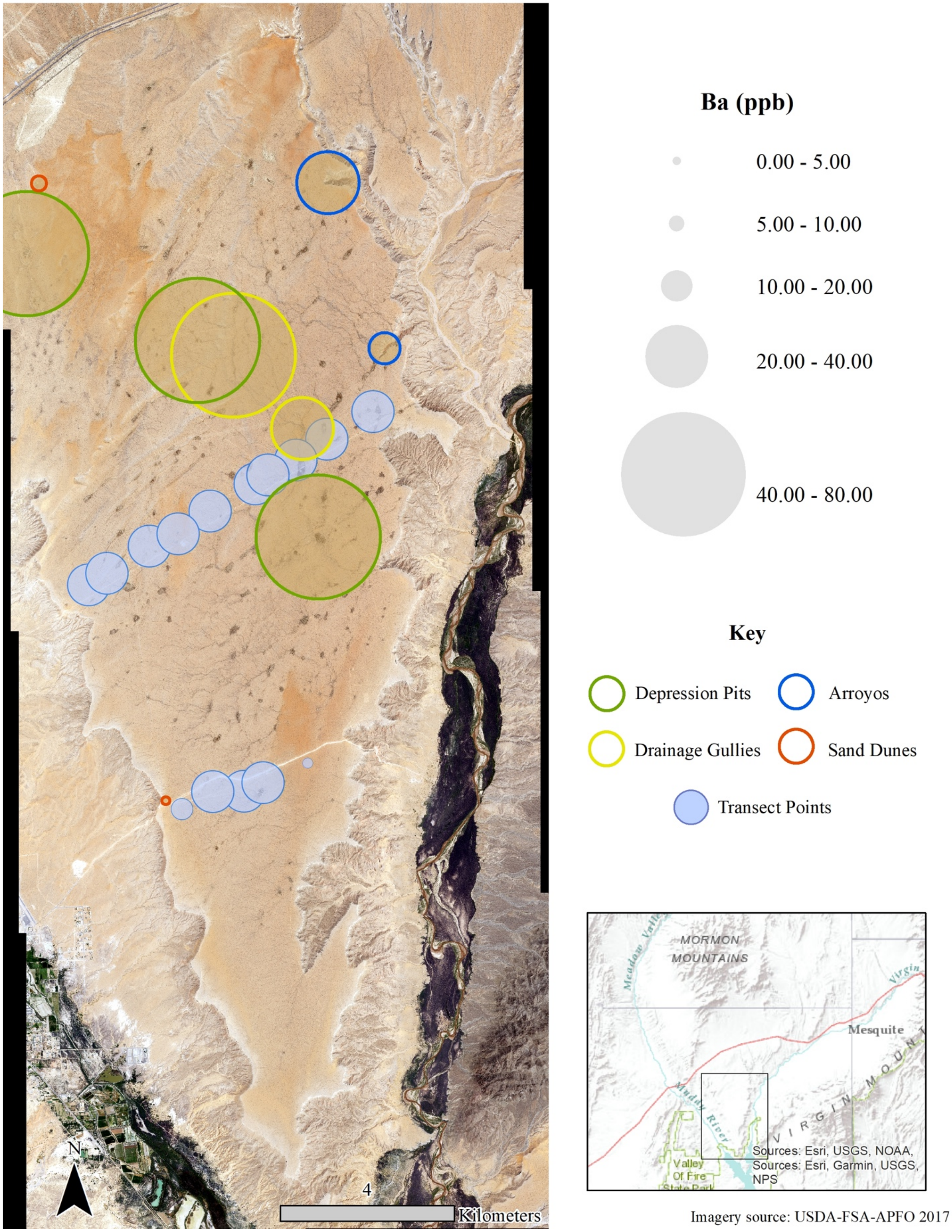

Figure 10: Ba (ppb) measurements along Mormon Mesa north and south transects and among geomorphic feature samples.

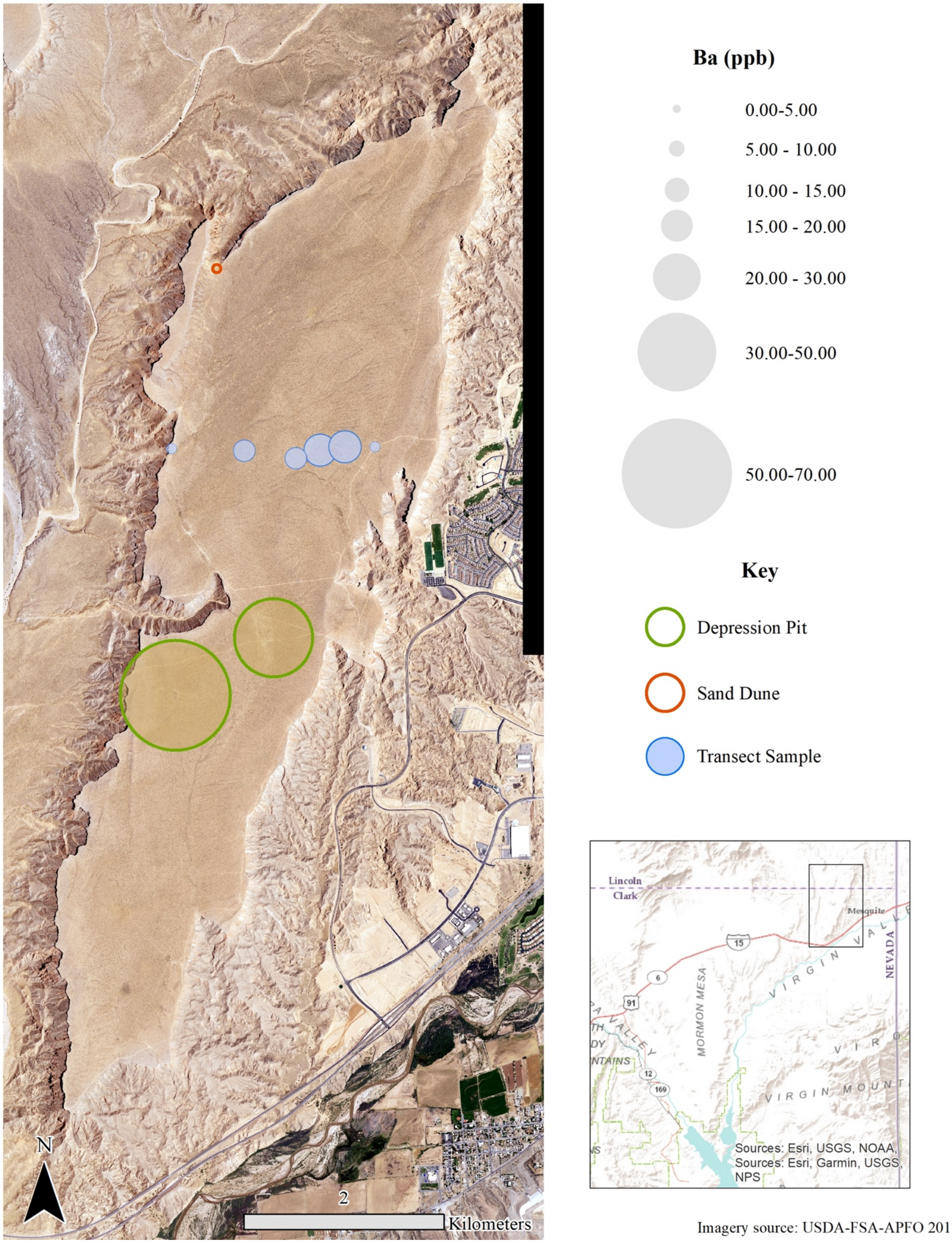

Figure 11: Ba (ppb) concentrations along Flat Top Mesa transect and among sand dune/depression pit samples.

Ba concentrations also varied among the soil horizon samples tested (Fig. 12 and Table 3). Both massive horizon samples tested returned very high Ba concentrations (131.9-244.24 ppb). The highest Ba concentrations throughout each profile were detected in the upper (max. 428.4 ppb) and middle (379.5 ppb) transitional horizon samples. Rubble horizon samples contained moderate Ba (41.95-53.78 ppb). The Muddy Creek parent material samples returned the lowest Ba ppb values (max. 11.74).

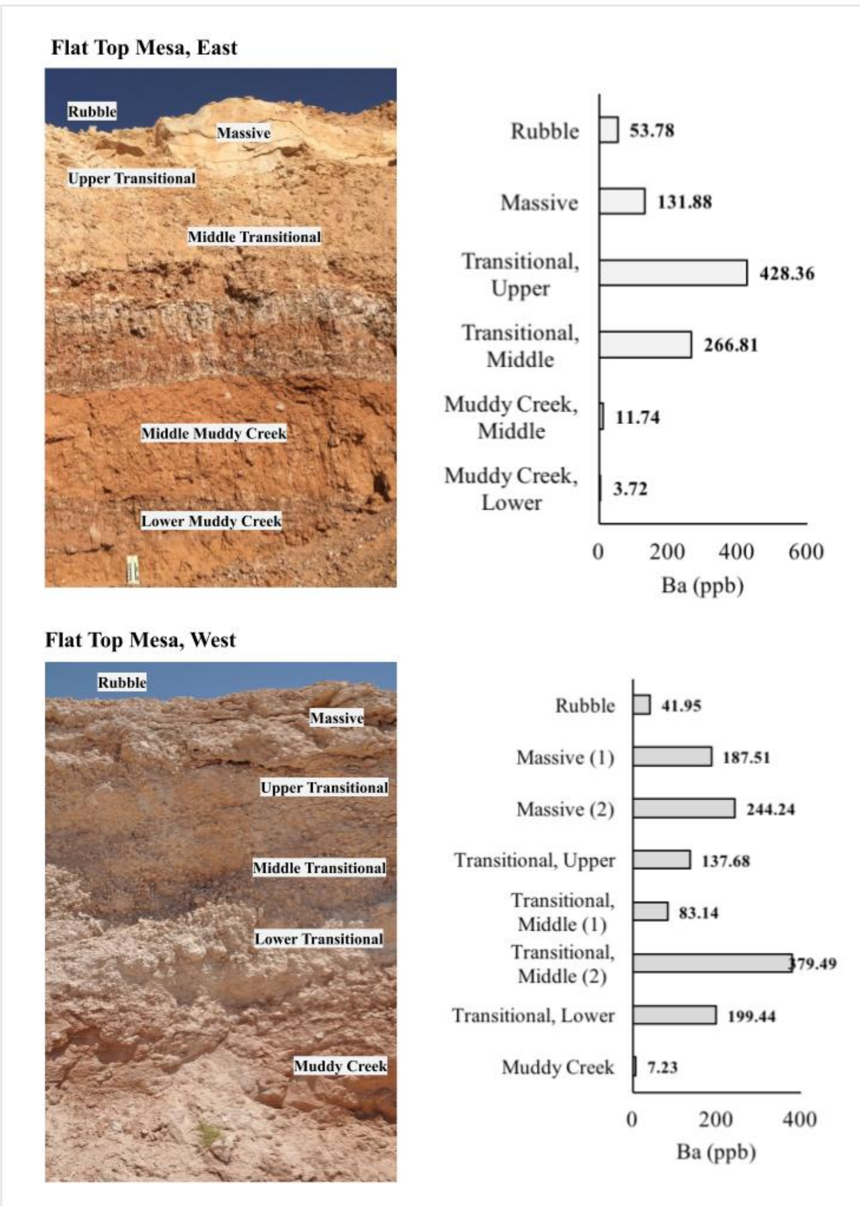

Figure 12: Ba concentrations (ppb) between soil horizons, Flat Top East and West

Table 3: Selected elemental concentrations (ppb) among soil horizons, Flat Top Mesa East and West profiles.

Sample Code	Sample Type	Location	Mn	Ba	Fe	K	Al
FTME2018IFR	Rubble	Flat Top East	50.78	53.78	2706.00	283.04	1813.87
FTME2018IFM	Massive	Flat Top East	15.67	131.88	1392.38	119.55	1051.73
FTME2018IFB	Transitional, Lower	Flat Top East	255.35	266.81	667.86	63.99	937.62
FTME2018IFC	Transitional, Upper	Flat Top East	6.45	428.36	564.42	34.36	892.23
FTMW2018IFTB	Transitional, Middle	Flat Top East	22.48	83.14	2905.18	595.89	1754.39
FTME2018IFA1b	Muddy Creek	Flat Top East	153.70	259.50	6641.41	601.90	3811.57
FTME2018IFA1c	Muddy Creek	Flat Top East	47.23	3.72	4059.38	243.16	1531.57
FTME2018IFA2c	Muddy Creek	Flat Top East	117.34	11.74	7004.33	723.12	5698.31
FTME2018IFA2d	Muddy Creek	Flat Top East	67.27	127.72	6353.19	610.35	4685.69
FTMW2018IFR	Rubble	Flat Top West	177.38	41.95	5889.68	451.25	3273.10
FTMW2018IFCF2L	Massive	Flat Top West	18.08	187.51	1703.98	234.49	1108.57
FTMW2018IFCF1	Massive	Flat Top West	829.80	244.24	1733.07	618.26	1251.98
FTMW2018IFTA	Transitional, Lower	Flat Top West	15.08	199.44	1945.19	133.39	1714.94
FTMW2018IFTC	Transitional, Upper	Flat Top West	17.40	137.68	2156.28	970.70	1848.93
FTMW2018IFTL	Transitional, Middle	Flat Top West	378.54	379.49	1389.66	1176.40	1278.33
FTMW2018IFMC	Muddy Creek	Flat Top West	15.86	7.23	1196.95	171.07	1355.83

Plotting Ba measurements in ppb against the measured concentrations of other elements produced mainly inconclusive results with the notable exceptions of Mn and Mg, the concentrations of which appear to be positively correlated with Ba concentration (see Fig. 13).

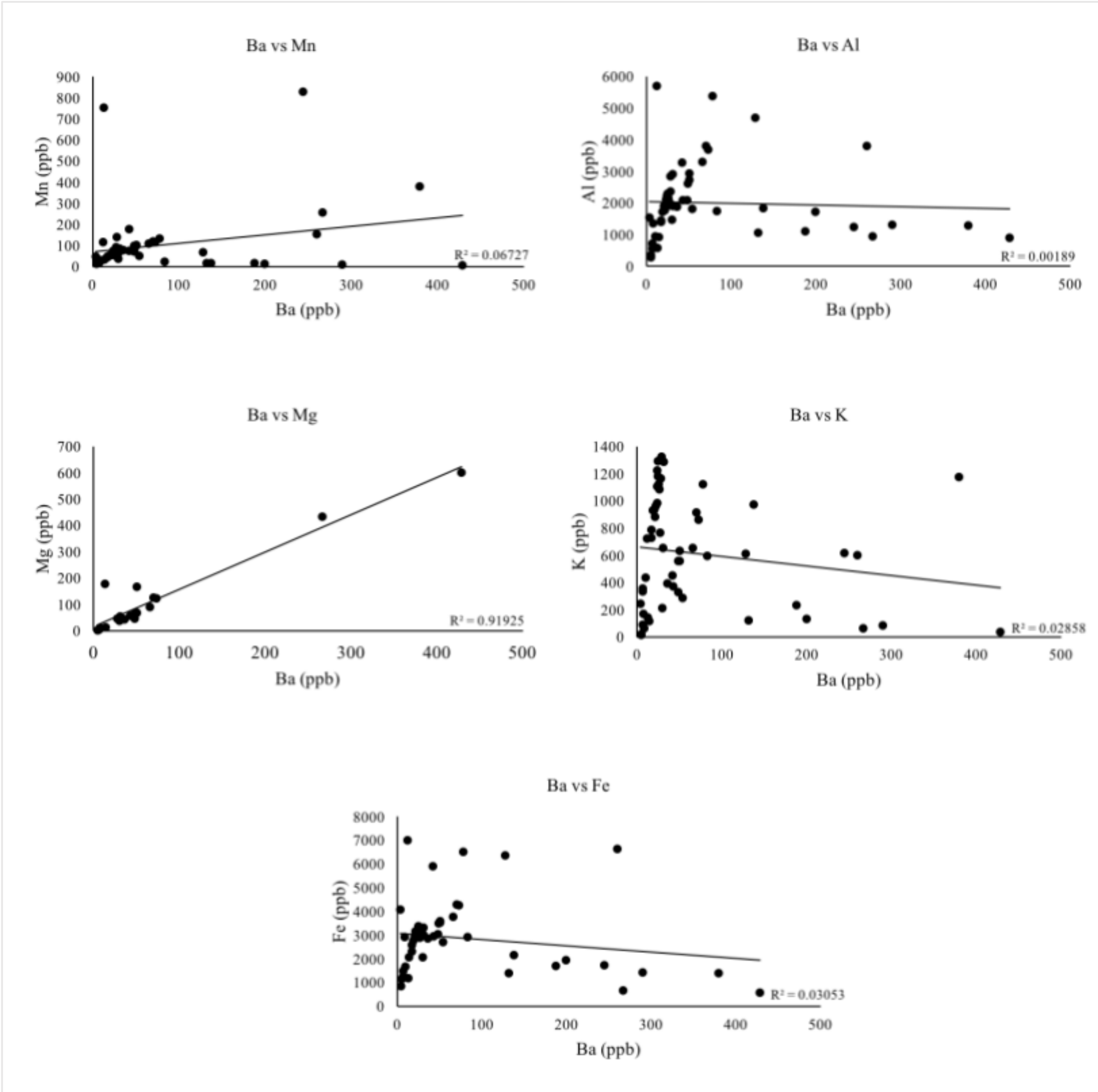

Figure 13: Results of plotting Ba (ppb) concentrations against concentrations of additional elements in samples to determine potential ion mobility pathways. Positive correlations appear to exist between Mn/Mg and Ba concentrations. Other linear fits yield inconclusive relationships.

DISCUSSION

Preliminary ICP-MS results of Ba and other elemental concentrations present a puzzle. The high Ba concentrations (as much as 428.4 ppb) detected in the massive and middle/upper transitional horizons of the soil are consistent with previously published observations of barite crystals in these horizons based on SEM imagery (Brock-Hon et al., 2012). These high Ba concentrations are likely the result of continuous accumulation of atmospherically-sourced ions in geomorphologically stable, relatively shallow horizons over an extended period of time. As an actively eroding surface (as evidenced by the presence of drainage networks, depression pits, arroyos, and reworked massive horizons clasts), the uppermost rubble layer of the Mormon Mesa soil sequence would not be able to accumulate much atmospherically-sourced Ba. Additionally, according to the eolian/atmospherically-sourced Ba hypothesis, with increasing profile depth one would expect decreasing Ba concentrations, as the translocated ions are sequestered in the shallower horizons. The low concentrations of Ba in the Muddy Creek and lower transitional horizons are consistent with this hypothesis. That the highest concentrations of Ba between both profiles were detected in the transitional subhorizons may be indicative of a maximum wetting depth within the soil profile, where ion concentrations could be particularly high if downward transport of atmospherically-sourced ions is indeed the primary barium input mechanism.

Relatively high concentrations of Ba among depression pit samples may point to the significance of hydrology in modern Ba solubility trends. As fluid collection points within an apparent hydrological network of drainage gullies on the mesa surface, the pits are likely to have more concentrated dissolved ions. These may prove to be ideal circumstances for increasing barium solubility, explaining why the data show somewhat elevated Ba concentrations among these samples, and also accounting for the lower Ba concentrations in drainage gully samples. If Ba was primarily sourced from the Muddy Creek Formation, surface concentrations in the soil would be low relative to those in the underlying parent materials. Future studies should investigate the influence of biologically-precipitated minerals on elemental concentrations in these sporadically moistened locations.

The apparently very low elemental concentrations among sand dune samples may be attributed to the fact that substrate samples, composed mainly of silicate minerals, were not digested in hydrofluoric acid. Complete digestions of all samples would yield more accurate data, and should be pursued in subsequent studies.

The lack of consistency in geochemical makeup of both arroyo samples may be due to the active erosion occurring at these sites. Active erosion would likely result in a chaotic mixing of lithic fragments, soil horizon materials, and transported grains, producing somewhat outlier results.

The relatively high Ba concentration in the playa sample may support the eolian hypothesis as well, as the fine evaporitic sediments in playas to the west of the mesa may have been blown onto the mesa surface. However, wind currently travels primarily in the northeast direction (National Digital Forecast Database, 2019) in the Mormon Mesa area, and may therefore be transporting ions from a host of other sources, the localities and geochemistry of which are beyond the scope of this study. That being said, there does not appear to be a WSW-increasing trend in Ba concentration from either Mormon Mesa or Flat Top Mesa transect samples. This may be due to shifts in wind direction over time which would result in a chaotic mixing of surface sediments with no apparent spatial gradient. Other geomorphological processes, including biological activity and fluid transport, may also affect Ba concentrations in surface samples, which could obfuscate eolian-driven spatial variations in geochemistry.

Ba concentrations were plotted against the measured concentrations of Mn, Mg, Al, K, and Fe with the goal of identifying potential relationships between Ba solubility and the presence of other ions. The apparent positive correlation between Mg and Ba concentration is consistent with experimental evidence indicating the increased solubility of Ba in the presence of Mg

(Deutsche, 1997). The weakly positive correlation between Mn and Ba concentrations warrants further investigation, as this may be indicative of Ba sourcing from hollandite, an Mn-oxide. While the concentration of Ba seems to be independent of the concentrations of K, Fe, and Al, the broad range of values for K, Fe, and Al ppb should be investigated, as these elements may also serve as indicators of climatic or geomorphic processes.

Future studies should sample additional adjacent playas, especially those south/southwest of the mesas, for more comprehensive geochemical data that may point to eolian transport of ions. Additionally, careful examinations of Na concentrations – spatially across the mesa surface, among geomorphic features, and throughout the profile – should be undertaken to assess the role of sodium content on the solubility of Ba in this particular environment. Complete digestions (in HF) should be carried out, especially for siliceous sand dune and Muddy Creek samples, to glean more accurate geochemical data. Additionally, dust flux should be measured at Mormon Mesa and the elemental makeup of dust samples analyzed to determine the specific content of aeolian inputs to the mesa surface.

CONCLUSION

This study incorporated data from ancient soil horizons as well as geomorphically active surface sediments to investigate the potential sources of Ba for authigenic barite found in the Mormon Mesa soil (Brock-Hon et al., 2012). By mapping the spatial variations in the concentration of barium and other associated elements in surface and profile samples, relationships between geomorphic features and chemical composition could be illuminated. ICP-MS data suggest that Ba ions are most concentrated in the transitional and massive horizons of the soil profile, as well as in the depression pits that dot the mesa surface. These trends, taken into consideration with the significance of dust flux in the study area, support the aeolian-transported barium hypothesis. Elevated Ba concentrations in depression pit samples may also suggest a hydrological component to barite neoformation in Mormon Mesa soils. Identifying the mechanisms that drive barite authigenesis can deepen our understanding of soil formation and ion mobilization, as well as allow us to anticipate the geochemical impacts of climate change on our soils.

REFERENCES

Blount, C. (1977). Barite solubilities and thermodynamic quantities up to 300 C and 1400 bars. *American Mineralogist, 62*, 942-947.

Brock, A., and Buck, B.J. (2009). Polygenetic development of the Mormon Mesa, NV petrocalcic horizons: geomorphic and paleoenvironmental interpretations. *Catena, 77(1)*, 65-75.

Brock-Hon, A., Robins, C.R., & Buck, B.J. (2012). Micromorphological investigation of pedogenic barite in Mormon Mesa petrocalcic horizons, Nevada USA: Implication for genesis. *Geoderma, 179-180*, 1-8.

Darmody, R.G., Harding, S.D., and Hassett, J.J. (1989). Barite authigenesis in surficial soils of mid-continental United States. In *Rock-Water Interaction* (Ed. D.L. Miles), pp. 183-186. WRI-6, A.A. Balkema, Rotterdam.

Deutsche, W.J. (1997). Groundwater geochemistry: Fundamentals and applications to contamination. Lewis Publ., Boca Raton, FL.

Gardner, L. (1972). Origin of the Mormon Mesa Caliche, Clark County, Nevada. *Geological Society of America Bulletin, 83*, 143-156.

Garvie, L., Burt, D., & Buseck, P. (2008). Nanometer-scale complexity, growth, and diagenesis in desert varnish. *Geology, 36*(3), 215-218.

Johnson, C.A., Piatak, N.M., and Miller, M.M. (2017). Barite (Barium), chap. D *of* Schulz, K.J., DeYoung, J.H., Jr., Seal, R.R., II, and Bradley, D.C., eds., Critical mineral resources of the United States – Economic and environmental geology and prospects for future supply: *U.S. Geological Survey Professional Paper 1802,* p. D1-D18.

Machette, M. (1985). Calcic soils of the southwestern United States. *Geological Society of America Special Paper, 203*, 1-21.

National Digital Forecast Database (2019). [Interactive wind speed/direction map]. *Wind Map.* Retrieved from http://hint.fm/wind/.

Reheis, M.C. (2006). A 16-year record of eolian dust in Southern Nevada and California, USA: Controls on dust generation and accumulation. *Journal of Arid Environments, 67*, 487-520.

Reheis, M., Budahn, J., & Lamothe, P. (2002). Geochemical evidence for diversity of dust sources in the southwestern United States. *Geochimica et Cosmochimica Acta, 66*(9), 1569-1587.

Reheis, M., Budahn, J., Lamothe, P., & Reynolds, R. (2009). Compositions of modern dust and surface sediments in the Desert Southwest, United States. *Journal of Geophysical Research, 114*, 1-20.

Reheis, M., Goodmacher, J., Harden, J., McFadden, L., Rockwell, T., Shroba, R., . . . Taylor, E. (1995). Quaternary soils and dust deposition in southern Nevada and California. *GSA Bulletin, 107*(9), 1003-1022.

Robins, C., Brock-Hon, A., & Buck, B. (2012). Conceptual Mineral Genesis Models for Calcic Pendants and Petrocalcic Horizons, Nevada. *Soil Science Society of America Journal*, 1-17.

Scott, A.J. (1988). The Muddy Creek Formation: Depositional environment, provenance, and tectonic significance in the western Lake Mead area, Nevada and Arizona. *UNLV Retrospective Theses & Dissertations, 9.*

Stoops, G., & Zavaleta, A. (1978). Micromorphological evidence of barite neoformation in soils. *Geoderma, 20*, 63-70.

APPENDIX A – EPA Method 3050B Section 7.5

NOTE: Section 7.5 may be used to improve the solubilities and recoveries of antimony, barium, lead, and silver when necessary. These steps are optional and are not required on a routine basis.

7.5 Add 2.5 mL conc. HNO3 and 10 mL conc. HCl to a 1-2 g sample (wet weight) or 1 g sample (dry weight) and cover with a watchglass or vapor recovery device. Place the sample on/in the heating source and reflux for 15 minutes.

7.5.1 Filter the digestate through Whatman No. 41 filter paper (or equivalent) and collect filtrate in a 100-mL volumetric flask. Wash the filter paper, while still in the funnel, with no more than 5 mL of hot (~95EC) HCl, then with 20 mL of hot (~95EC) reagent water. Collect washings in the same 100-mL volumetric flask.

7.5.2 Remove the filter and residue from the funnel, and place them back in the vessel. Add 5 mL of conc. HCl, place the vessel back on the heating source, and heat at 95EC ± 5EC until the filter paper dissolves. Remove the vessel from the heating source and wash the cover and sides with reagent water. Filter the residue and collect the filtrate in the same 100-mL volumetric flask. Allow filtrate to cool, then dilute to volume. NOTE: High concentrations of metal salts with temperature-sensitive solubilities can result in the formation of precipitates upon cooling of primary and/or secondary filtrates. If precipitation occurs in the flask upon cooling, do not dilute to volume.

7.5.3 If a precipitate forms on the bottom of a flask, add up to 10 mL of concentrated HCl to dissolve the precipitate. After precipitate is dissolved, dilute to volume with reagent water. Analyze by FLAA or ICP-AES.

NB: Step 7.5.2 was not used in this experiment.

APPENDIX B – Standard elemental concentrations

Relevant elemental concentrations in standards used for ICP-MS analysis. Figures listed without % are in ppb.

Element	SRM 2586	WPS1	WPS3
Mn	1000	100	N/A
Ba	413	N/A	500
Fe	5.16%	100	N/A
K	0.98%	N/A	100
Al	6.65%	500	N/A
Mg	1.71%	N/A	100